2000

X-ray Standing-Wave Investigation of (1X2)Rb/Cu(110)

David R. Heskett
University of Rhode Island, dheskett@uri.edu

L. E. Berman

Citation/Publisher Attribution

Heskett, D. and L. E. Berman. "X-Ray Standing-Wave Investigation of (1X2)Rb/Cu(110)." Physical Review. B. Condensed Matter. 61(12):8450-8454. 15 March 2000.
Available at http://link.aps.org/doi/10.1103/PhysRevB.61.8450

X-ray standing-wave investigation of (1×2)Rb/Cu(110)

D. Heskett
Department of Physics, University of Rhode Island, Kingston, Rhode Island 02881

L. E. Berman
National Synchrotron Light Source, Brookhaven National Laboratory, Upton, New York 11973

(Received 11 October 1999)

We have carried out a back-reflection x-ray standing-wave (BRXSW) investigation to study the adsorbate ordering in the system (1×2)Rb/Cu(110), which corresponds to an alkali-induced missing row reconstruction of the Cu(110) surface. By carrying out measurements in three different scattering geometries, we find that for the missing row structure at room temperature, the Rb adatoms are extremely well ordered in the direction perpendicular to the surface, show a high degree of ordering across the missing rows (e.g., the atoms are locked into the missing row troughs), but are highly disordered along the rows, similar to a one-dimensional lattice gas. We compare our results to the Rb/Cu(110)-saturated surface at room temperature and to our previous BRXSW investigation of Rb/Cu(111).

I. INTRODUCTION

The alkali-induced (1×2) reconstructions of the (110) surfaces of fcc metal crystals have been extensively investigated as prototypic examples of adsorbate-induced surface reconstructions.[1–3] It has been demonstrated by a variety of surface structural probes that for the (1×2) overlayer the alkali adatoms induce a missing (or added) row reconstruction of the substrate surface, with every other close-packed row removed due to the adsorption of the alkali adatoms (see Fig. 1). It is generally assumed that the alkali atoms reside in the surface troughs created by the missing rows. Since the (1×2) diffraction pattern is caused by the substrate surface, not by the alkali atoms, less is known in detail about the geometric and structural parameters of the alkali atoms themselves. The x-ray standing-wave technique (XSW) has elemental specificity and is also a local structural probe, so its structural information is not limited by the diffraction pattern of the substrate.[4–7] As such, it is a very useful technique for probing the geometry and structural parameters of the alkali adatoms in such a system.

During Bragg diffraction from a single crystal, the incident and reflected x-ray plane waves interfere to set up a standing wave field parallel to and having the same spatial periodicity as the diffraction planes. When the scattering angle or photon energy is scanned through the finite range of the total reflectivity condition, the phase of this standing-wave field, and therefore the x-ray intensity maximum, shifts continuously relative to the atomic scattering planes. By measuring a yield characteristic of an adsorbate excited by the standing-wave field, such as Auger, photoemission, or x-ray fluorescence, the atom's position and degree of order relative to the diffraction planes can be determined. The adsorbate's bonding site can also be determined with geometric triangulation by combining results of standing-wave measurements using sets of diffraction planes that are not parallel. In the present paper we have performed back-reflection XSW (BRXSW) measurements in several different scattering geometries to probe the ordering of the Rb atoms in the system (1×2)Rb/Cu(110).

II. EXPERIMENT

The experiments reported below were performed on beamline X24A at the National Synchrotron Light Source at Brookhaven National Laboratory. This beamline is UHV compatible to allow windowless operation for improved flux at low photon energies.[8] X-ray photons from the storage ring were monochromatized using a double-crystal assembly, with either Si(111) or Si(220) diffracting crystals, and focused onto the sample by a toroidal nickel-coated quartz mirror. The UHV chamber which we attached to this beamline was equipped with a cylindrical mirror analyzer, sputter ion gun, alkali evaporator, and other standard UHV instrumentation; a base pressure in the low 10^{-10} Torr range was achieved.

The Cu(110) sample was cleaned by Ar^+ sputtering and was annealed to 700 K for 5 min. The crystal was clamped onto a tantalum plate attached to a button heater which was used to raise the temperature of the sample. A chromel-alumel thermocouple clamped to the crystal was used for temperature measurements. The Rb was evaporated from a commercial SAES Getter source equipped with a shutter and collimator. The (1×2) overlayer was produced by saturating the Cu(110) surface with Rb at room temperature (based on a leveling in the intensity of the Rb $2p$ core levels vs dose times), and then annealing the sample to $\sim$250 °C for 1 min. A low-energy electron diffraction (LEED) study at URI had shown that this procedure reproducibly produced a clear (1×2) LEED pattern. All XSW measurements reported here were performed at room temperature.

The BRXSW experiments were conducted by setting either the (220), (111), or (200) planes of the Cu(110) crystal perpendicular to the incident monochromatized x-ray beam. For the (220) reflection, the x-ray beam was incident normal to the sample surface. For the (111) and (200) reflections, the x-rays were incident at 35.3° and 45° to the surface normal

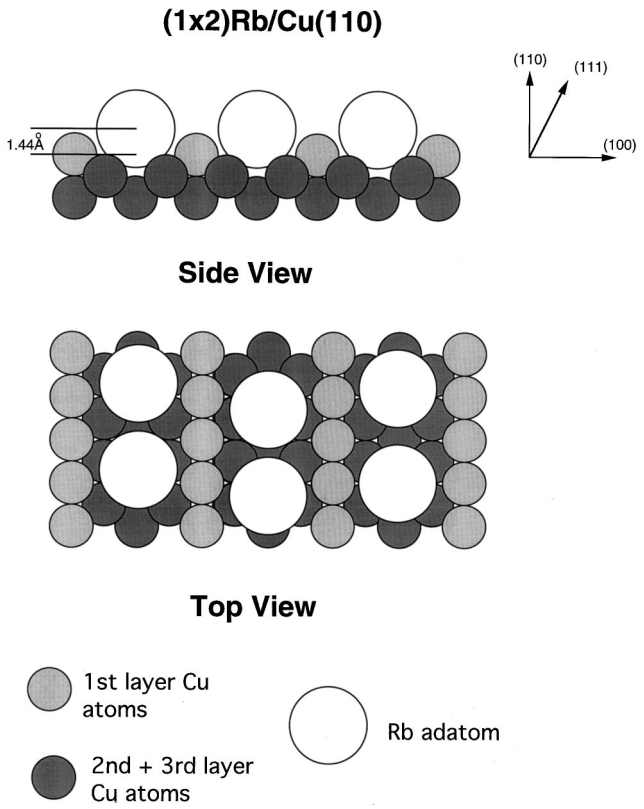

FIG. 1. Schematic illustration of the (1×2) missing row reconstruction of the Rb/Cu(110) surface.

along the [001] and $[\bar{1}10]$ directions in the substrate surface, respectively. For the XSW measurements, the photon energy was scanned around the following energies which coincided with the peaks of the crystal rocking curves: (220) geometry—4858 eV, (111) geometry—2970 eV; (200) geometry—3431 eV. In each case the XSW signal from the copper substrate was monitored by measuring the Cu LMM Auger electron yield at 920-eV kinetic energy as the photon energy was scanned through the Bragg rocking curves. The Rb signal was monitored by recording the intensity of either the Rb $2s$ or $2p$ core levels or one of the Rb LMM Auger peaks. Simultaneously with the XSW signal, the reflectivity was detected from the photocurrent generated on nickel grids in the incident and reflected beam paths.

III. RESULTS

In Fig. 2, we present an electron energy distribution curve of the region containing the Ni LMM and Rb $2p$ core-level peaks taken at a photon energy of 2975 eV ($\sim$5 eV higher than the peak of the rocking curve) in the (111) scattering geometry for the Cu(110) surface with one layer of rubidium deposited at room temperature. The collection of XSW data consists of recording the height of one of the Rb LMM Auger or core-level peaks (as in this case) as well as background points (at kinetic energies approximately 20 eV higher than the associated Auger or photoemission peaks) as the photon energy was scanned around the rocking curve, 3 eV on either side in 0.1 eV increments.

In Figs. 3–5 we present sample results of our XSW measurements for 1-ML Rb/Cu(110) in the (220), (111), and

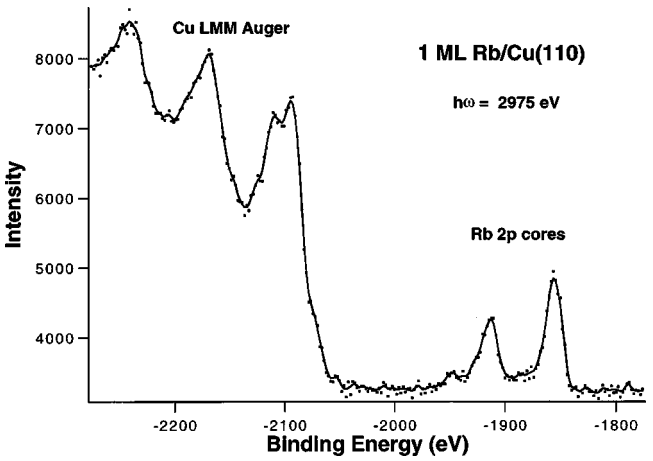

FIG. 2. Electron energy distribution curves for one monolayer of Rb on Cu(110) deposited at room temperature showing the Cu LMM and Rb $2p$ regions. The scattering geometry was the (111) geometry; the photon energy was 2975 eV.

(200) geometries, respectively. For each reflection plane, the lowest curve is the reflectivity and the upper one represents the appropriate Rb photoemission yield, normalized to unity away from the Bragg reflection. The solid lines are fits to the data. The reflectivity curves were reproduced by convoluting a Gaussian instrumental resolution function with the intrinsic Darwin-Prins reflectivity curve. This same Gaussian broadening was then used in fitting to the photoelectron and Auger yield data.

The adsorbate photoelectron yield in the standing-wave field is given by

$$Y(E)/Y_{0B}=1+R(E)+2\sqrt{R(E)}f\cos(\upsilon[E]-2\pi\phi).$$

Here the reflectivity is $R(E)=|(E_H/E_0[E])|^2$, where E_0 and E_H are the incident and diffracted beam electric-field amplitudes, respectively; $\upsilon[E]$ is the energy-dependent phase of E_H relative to E_0; Y_{0B} is the emission yield away from the Bragg reflection; and f and ϕ are the so-called coherent frac-

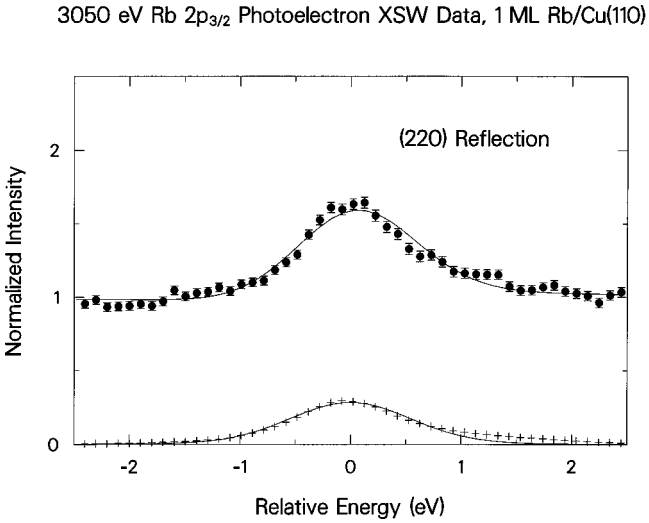

FIG. 3. Energy dependence of the Rb $2p_{3/2}$ photoelectron standing-wave yield in the (220) reflection plane for 1-ML Rb/Cu(110) (upper curve). The lower curve is the measured reflectivity and the solid lines are fits using dynamic diffraction theory.

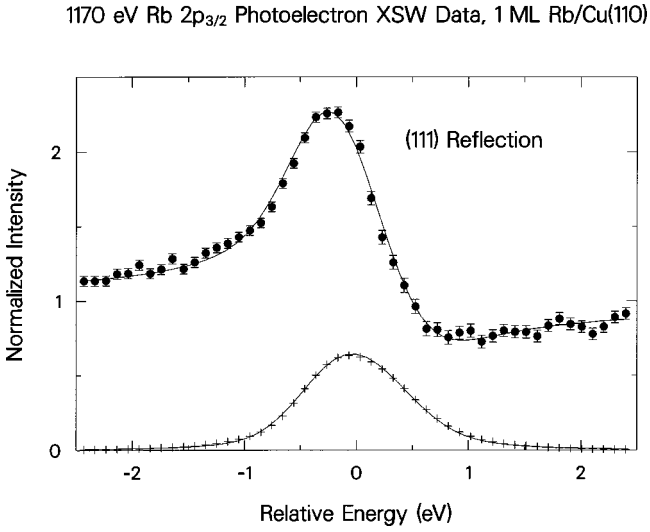

FIG. 4. Energy dependence of the Rb $2p_{3/2}$ photoelectron standing-wave yield in the (111) reflection plane for 1-ML Rb/Cu (110) (upper curve). The lower curve is the measured reflectivity and the solid lines are fits using dynamic diffraction theory.

tion and coherent position. They represent, respectively, the spread of positions taken on by the adsorbate atoms, and the weighted average position of the atoms relative to the diffraction planes. The coherent position takes on a value between 0 and 1, with a value of 0 or 1 corresponding to a position on the planes, and 1/2 corresponding to a position midway between the planes. The coherent fraction comprises the product of a thermal Debye-Waller factor for the adsorbate, a factor determined by static disorder, and a geometrical factor which includes the effect of multiple-site adsorption relative to the reflecting planes. A value of unity for the geometrical factor means that all the Rb atoms are located at the same (coherent) position relative to the diffraction planes, while a value of less than 1 for the coherent fraction means that more than one position is occupied or there is some type of disorder in the system.

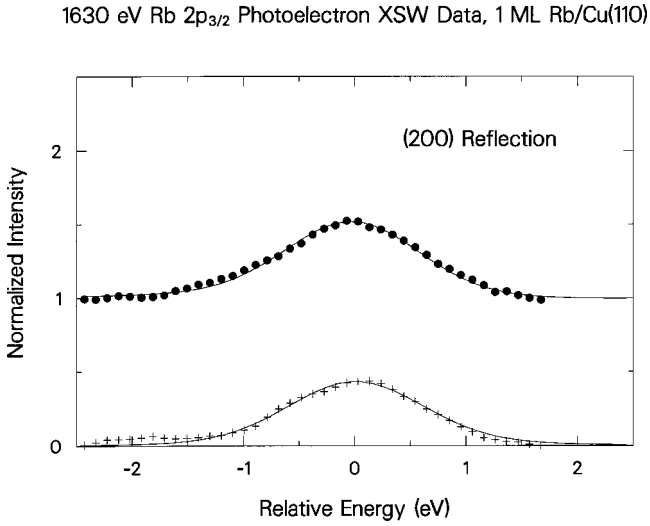

FIG. 5. Energy dependence of the Rb $2p_{3/2}$ photoelectron standing-wave yield in the (200) reflection plane for 1-ML Rb/Cu (110) (upper curve). The lower curve is the measured reflectivity and the solid lines are fits using dynamic diffraction theory.

TABLE I. Summary of XSW results for Rb/Cu(110). [Error bar on average=greater of (range/2) or (greatest individual uncertainty)].

Geometry	Overlayer	Coh. pos., ϕ	Coh. fract., f
(220)	(1×2)	0.148 ± 0.024	0.760 ± 0.13
		0.116 ± 0.015	0.675 ± 0.061
		0.114 ± 0.037	0.573 ± 0.121
Avg.		0.126 ± 0.037	0.67 ± 0.12
(220)	Saturation	0.178 ± 0.01	0.945 ± 0.08
		0.218 ± 0.006	0.718 ± 0.036
Avg.		0.198 ± 0.02	0.832 ± 0.11
(111)	(1×2)	0.463 ± 0.003	0.838 ± 0.018
		0.465 ± 0.003	0.772 ± 0.017
		0.460 ± 0.004	0.718 ± 0.017
Avg.		0.463 ± 0.004	0.776 ± 0.06
(111)	Saturation	0.415 ± 0.003	0.509 ± 0.01
		0.397 ± 0.003	0.603 ± 0.012
		0.426 ± 0.002	0.670 ± 0.011
Avg.		0.412 ± 0.014	0.594 ± 0.08
(200)	(1×2)	0.394 ± 0.009	0.221 ± 0.014
		0.379 ± 0.053	0.133 ± 0.033
		0.273 ± 0.009	0.201 ± 0.016
		0.303 ± 0.015	0.123 ± 0.017
Avg.		0.337 ± 0.06	0.170 ± 0.05
(200)	Saturation	0.352 ± 0.006	0.13 ± 0.004

Table I summarizes the coherent positions and coherent fractions from several separate data sets in the three geometries for the (1×2)Rb/Cu(110) overlayer. We also include data from saturation coverages of Rb at room temperature, for which we estimate the coverage to be approximately twice that of the (1×2) overlayer from relative core-level intensities. For the saturated overlayer we observed fairly disordered LEED patterns with streaky (1×3) and (4×4) spots.

IV. DISCUSSION

From the results summarized in Table I, it is clear that the Rb atoms are highly ordered for the (220) scattering geometry, which corresponds to a high degree of order perpendicular to the Cu(110) surface. This is true for both the (1×2) reconstructed surface and for the saturated layer. This might at first appear to be quite surprising since the saturated surface shows only a poorly ordered and mixed LEED pattern and the (1×2) LEED pattern corresponds to the substrate surface reconstruction and not to the overlayer (in other words, the Rb atoms themselves are not ordered in such a way that they exhibit a well-defined LEED pattern at room temperature).

On the other hand, these results are quite consistent with our previous BRXSW investigation of Rb/Cu(111) (Refs. 9, 10) in the sense that for all coverages, even lower coverages for which no distinct LEED pattern was detected at room temperature, we found that the Rb adatoms always exhibited high coherent fractions in the (111) geometry, corresponding to a high degree of ordering perpendicular to the Cu(111) surface. In addition, for the (1×2)Rb/Cu(110) overlayer, the

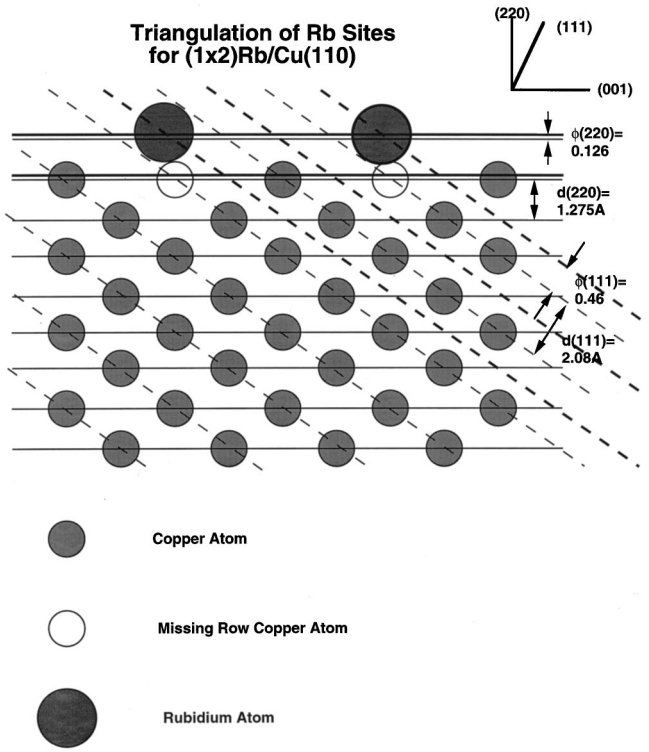

FIG. 6. Illustration of the triangulation of Rb positions using the (220) and (111) BRXSW results for the (1×2)Rb/Cu(110) overlayer (using the average values from Table I). The thin solid and dashed lines represent the (220) and (111) lattice planes, respectively. The thick solid and dashed lines represent the respective allowed coherent plane positions of the Rb atoms with respect to these planes. Rb adsorption sites are at the intersections of the coherent position planes, as shown.

perpendicular spacing (2.71 Å) (Ref. 11) of the Rb atoms from the midplane of the underlying copper surface corrugation (the second copper layer, as illustrated in Fig. 6) is very close to the perpendicular spacing previously found for the (2×2)Rb/Cu(111) overlayer (2.89 Å).[9,10] So for both systems the alkali atoms maintain a more or less uniform height above the surface, even for two quite different substrate surface configurations (close-packed surface vs open missing row surface).

For the (111) scattering geometry, the coherent fraction was high for both the (1×2) overlayer ($f\sim0.8$) and for the saturated surface ($f\sim0.6$). In this geometry, a component of the scattering is in the [001] direction in the surface, i.e., across the (1×2) missing rows. For the (1×2) case, the high coherent fraction is consistent with the Rb atoms being ''locked'' into the missing row troughs, as has been previously suggested by a number of investigators. It is not surprising that the (111) coherent fraction for the Rb/Cu(110) saturated layer (0.6) is lower compared with the (1×2) case (0.8) since the LEED pattern for the saturated surface was mixed and not very clear, already indicating some degree of disorder within this overlayer.

Using the results from the (220) and (111) measurements, we can triangulate to the positions of the Rb atoms in the direction across the rows for the (1×2) overlayer. As illustrated in Fig. 6, our results can be modeled by assuming a missing row model of the surface with the Rb atoms close to being centered in the missing rows but displaced above the surface layer by 1.44 ± 0.05 Å. For the saturated layer, the Rb atoms are situated at 1.53 ± 0.025 Å above the Cu(110) surface, according to the average (220) coherent position given in Table I. This slightly higher location compared with the (1×2) overlayer is reasonable since for the saturated surface we do not expect all of the atoms to be as firmly embedded in the Cu(110) missing row troughs.

It should be pointed out that the model and analysis presented in Fig. 6 assumed an unrelaxed and unreconstructed surface (aside from the missing rows). The XSW technique is not directly sensitive to any such surface changes. Measurements of alkalis/Cu(110) by other techniques have found relaxations of the top surface layer from 0% to -12% as well as additional displacements of surface and subsurface atoms in some cases.[12–15]. A relaxation of the top layer would not affect our XSW-inferred adsorption sites in the missing rows, but would modify the quoted Rb distance above the surface, and could also account for the different (220) coherent positions for the (1×2) and saturated surfaces.

The high (111) coherent fraction is consistent with a relatively high degree of order of Rb atoms within the missing rows. This should be contrasted with our study of Rb/Cu(111).[10] In a scattering geometry which probed the ordering of the Rb atoms parallel to the Cu(111) surface, we found very low coherent fractions for all coverages, indicating that the Rb atoms were in a highly disordered state parallel to the surface, even for the saturated layer which produced a distinct (2×2) LEED pattern.

Turning now to the (200) scattering geometry, we find very low coherent fractions for both the (1×2) and saturated overlayers. This indicates a high degree of disorder of the Rb atoms in the [110] direction in the surface, i.e., along the missing row troughs. This is consistent with the alkali atoms adsorbing in a disordered or liquidlike form within the missing row troughs. (Low coherent fractions can also be obtained from other configurations,[4,5,7] for example, with the occupation by the Rb atoms of two or more well-defined sites along the troughs. This alternative cannot be ruled out by our results.) These low coherent fractions are also very similar to the low coherent fractions for the Rb atoms in the direction parallel to the surface for Rb/Cu(111) (Ref. 10) at all coverages, as discussed above.

In summary, we have carried out a back-reflection x-ray standing-wave investigation to study the adsorbate ordering for the system (1×2)Rb/Cu(110), which corresponds to an alkali-induced missing row reconstruction of the Cu(110) surface. We find that for the missing row structure at room temperature, the Rb adatoms are extremely well ordered in the direction perpendicular to the surface, show a high degree of ordering across the missing rows, but are highly disordered along the rows.

ACKNOWLEDGMENTS

This research was carried out at the National Synchrotron Light Source at Brookhaven National Laboratory, which is

sponsored by the U.S. Department of Energy through Contract No. DE-AC02-76CH0006. We would like to thank B. Karlin for his assistance at beamline X24A. We would also like to thank Dr. D. Zehner for providing the Cu(110) crystal used in this experiment. D. Heskett acknowledges the Donors of the Petroleum Research Fund, administered by the American Chemical Society, for partial support of this research.

[1] T. Aruga and Y. Murata, Prog. Surf. Sci. **31**, 61 (1989).
[2] *Physics and Chemistry of Alkali Metal Adsorption*, edited by H. P. Bonzel, A. M. Bradshaw, and G. Ertl (Elsevier, Amsterdam, 1989), pp. 111–128.
[3] E. H. Conrad and H. Hornis, Prog. Surf. Sci. **48**, 221 (1995).
[4] J. Zegenhagen, Surf. Sci. Rep. **18**, 199 (1993).
[5] D. P. Woodruff, Prog. Surf. Sci. **57**, 1 (1998).
[6] D. P. Woodruff, D. L. Seymour, C. F. McConville, C. E. Riley, M. D. Crapper, N. P. Prince, and R. G. Jones, Surf. Sci. **195**, 237 (1988).
[7] D. P. Woodruff, B. C. C. Cowie, and A. R. H. F. Ettema, J. Phys.: Condens. Matter **6**, 10 633 (1994).
[8] P. L. Cowan, S. Brennan, R. D. Deslattes, A. Henins, T. Jach, and E. G. Kessler, Nucl. Instrum. Methods Phys. Res. A **246**, 154 (1986).
[9] X. Shi, C. Su, D. Heskett, L. Berman, C.-C. Kao, and M. J. Bedzyk, Phys. Rev. B **49**, 14 638 (1994).
[10] D. Heskett, P. Xu, L. Berman, C.-C. Kao, and M. J. Bedzyk, Surf. Sci. **344**, 267 (1995).
[11] The Rb-copper lattice plane perpendicular distance, d, for the (1×2)Rb/Cu(110) overlayer using the average (220) coherent position from Table I (0.126) and the geometry illustrated in Fig. 6 is given by $d=(0.126)(1.275\ \text{Å})+(2)(1.275\ \text{Å})=2.71\ \text{Å}$.
[12] R. D. Diehl and R. McGrath, Surf. Sci. Rep. **23**, 43 (1996).
[13] Z. P. Hu, B. C. Pan, W. C. Fan, and A. Ignatiev, Phys. Rev. B **41**, 9692 (1990).
[14] Ph. Hofmann, S. Bao, K.-M. Schindler, O. Schaff, M. Polcik, V. Fritzsche, A. M. Bradshaw, R. Davis, and D. P. Woodruff, Surf. Sci. **319**, L7 (1994).
[15] R. Schuster and I. K. Robinson, Phys. Rev. Lett. **76**, 1671 (1996).